Available online at www.sciencedirect.com
ScienceDirect
Journal of Catalysis 249 (2007) 15–23
JOURNAL OF CATALYSIS
www.elsevier.com/locate/jcat

Lanthanum-doped zinc hydroxycarbonates for the catalytic disproportionation of hydrogen peroxide into singlet oxygen

Joos Wahlen [a], Dirk E. De Vos [a,*], Pierre A. Jacobs [a], Véronique Nardello [b], Jean-Marie Aubry [b], Paul L. Alsters [c]

[a] *Centre for Surface Chemistry and Catalysis, K.U. Leuven, Kasteelpark Arenberg 23 Box 2461, 3001 Leuven, Belgium*
[b] *LCOM, Equipe de Recherches "Oxydation et Formulation", UMR CNRS 8009, ENSCL, BP 90108, F-59652 Villeneuve d'Ascq Cedex, France*
[c] *DSM Pharmaceutical Products—Advanced Synthesis, Catalysis and Development, P.O. Box 18, 6160 MD Geleen, The Netherlands*

Received 10 January 2007; revised 14 March 2007; accepted 16 March 2007

Available online 16 May 2007

Abstract

Lanthanum-containing materials were obtained by coprecipitation of La^{3+} and Mg^{2+}, Ca^{2+}, or Zn^{2+} in the presence of sodium carbonate. All materials were tested in the disproportionation of hydrogen peroxide into singlet molecular oxygen ($^1O_2$). Whereas La supported on Mg or Ca hydroxycarbonate showed very low catalytic activity, La-doped zinc hydroxycarbonate was far more active, even without addition of a soluble base. This may be related to the high surface area and small crystal size of the Zn material and the high number of easily accessible basic sites. The catalytic performance of a series of La-containing Zn hydroxycarbonates with varying La/Zn ratios was strongly dependent on the composition; the highest catalytic activity was observed for materials having relatively small amounts of La. Structural characterization of the materials revealed that at low La content, the Zn–La coprecipitate can be considered a Zn hydroxycarbonate (hydrozincite) doped with a small amount of La. At higher La content, distinct La (hydroxy)carbonate phases are formed, which are less active in the disproportionation of H_2O_2. Filtrate tests demonstrated that the La-doped Zn hydroxycarbonate is a truly heterogeneous catalyst, allowing recycling of the catalyst. Finally, this material was used for the selective peroxidation of functionalized alkenes. After reduction of the hydroperoxides, the corresponding allylic alcohols were obtained in good chemical yield (>90%).

Keywords: Heterogeneous catalysis; Hydrogen peroxide; Hydroperoxides; Hydrotalcites; Hydroxycarbonates; Hydrozincite; Lanthanum; Oxidation; Singlet oxygen; Zinc

1. Introduction

Singlet molecular oxygen ($^1O_2$) is a valuable reagent in organic synthesis. This electrophilic two-electron oxidant shows unique nonradical reactivity and high chemoselectivity [1]. For instance, reaction of $^1O_2$ with electron-rich alkenes yields allylic hydroperoxides, which can be converted to synthetically useful allylic alcohols [2].

The most frequently used method for the production of $^1O_2$ is the photosensitization of triplet molecular oxygen [3,4]. Alternatively, singlet oxygen can be generated from hydrogen peroxide in the presence of a metal catalyst,

$$2H_2O_2 \xrightarrow{\text{catalyst}} {}^1O_2 + 2H_2O.$$

Several inorganic compounds (e.g., Mo, W, La, Ca) are known to catalyze the disproportionation of H_2O_2 [5]. Molybdenum is often the preferred catalyst because it generates $^1O_2$ with high H_2O_2 efficiency under mild reaction conditions [6–8]; for instance, homogeneous molybdate (MoO_4^{2-}) in aqueous solvents or microemulsions has been used for the peroxidation of olefinic compounds [9–11]. On the other hand, highly active, heterogeneous Mo catalysts have been prepared by immobilization of MoO_4^{2-} on anionic clays [12–16]. Recently, the use of lanthanum(III) hydroxide and La-exchanged zeolites has been reported for the catalytic disproportionation of H_2O_2 into singlet oxygen [17–20]. Although lanthanum shows lower activity

* Corresponding author. Fax: +32 16 32 1998.
E-mail address: dirk.devos@biw.kuleuven.be (D.E. De Vos).

0021-9517/$ – see front matter
doi:10.1016/j.jcat.2007.03.017

and less efficient use of H_2O_2 compared with molybdenum, La has some advantages in the selective oxidation of allylic alcohols and certain allylic amines [17,21]. These reactions cannot be carried out using conventional Mo catalysts, due to competing epoxidation of the double bond or *N*-oxidation by the direct reaction of the Mo-peroxo species with these functional groups. In contrast, La-peroxo species themselves show no reactivity toward these functions.

But the catalytic activity of lanthanum hydroxide is rather low, presumably because most of the lanthanum is buried in the inactive bulk phase. Consequently, only a small number of the La ions are catalytically active. The immobilization of La on zeolites results in improved activity, but the micropores within the zeolites may induce enhanced quenching of $^1O_2$ or may hinder the diffusion of bulky olefins. On the other hand, zeolites are rather expensive materials, and these catalysts are active only if a soluble base like sodium hydroxide is added [18,19]. In this study, we prepared lanthanum-containing materials by simple coprecipitation of La^{3+} and Mg^{2+}, Ca^{2+}, or Zn^{2+} with sodium carbonate and evaluated the catalytic activity of the resulting materials in the disproportionation of hydrogen peroxide into singlet oxygen.

2. Experimental

2.1. Materials

All materials were obtained from commercial sources and used without purification. $La(OH)_3$ and La_2O_3 were obtained from Aldrich and Acros, respectively. Hydrogen peroxide was a 50 wt% aqueous solution obtained from Acros. Commercial 30 and 50 wt% H_2O_2 could be used interchangeably, providing similar results. (Caution: H_2O_2 and alkyl hydroperoxide solutions are strongly oxidizing and should be handled with appropriate precautions.)

2.2. Synthesis and characterization of lanthanum-containing materials

2.2.1. Coprecipitation of lanthanum and zinc

In a typical synthesis, a La-doped Zn hydroxycarbonate (La/Zn ratio = 10/90, La[10]Zn[90]) was prepared by coprecipitating La^{3+} and Zn^{2+} nitrate salts with Na_2CO_3. In a 500-mL round-bottomed flask, 0.045 mol $Zn(NO_3)_2{\cdot}6H_2O$ and 0.005 mol $La(NO_3)_3{\cdot}6H_2O$ were dissolved in 100 mL of deionized water, and the solution was heated to 80 °C. Next, a solution of 0.066 mol Na_2CO_3 in 50 mL of deionized water was added to the La–Zn solution at a constant rate of 100 mL h^{-1}. After the addition of Na_2CO_3, the mixture was stirred for another 1 h. The suspension was then cooled to room temperature, and the white precipitate was centrifuged (10 min at 3500 rpm) and washed/centrifuged three times with deionized water (3 × 150 mL). Finally, the material was dried by lyophilization. Subsequently, 150 mL of deionized water was added to the solid, and the resulting suspension was freeze-dried in a 1-L flask. This material was designated La[10]Zn[90].

The same procedure was used for the preparation of La-containing materials with different La/Zn molar ratios (La/Zn = 0/100, 1/99, 5/95, 25/75, 50/50, and 100/0) by varying the relative concentrations of the La and Zn salts. The amount of Na_2CO_3 was adjusted to maintain the Na_2CO_3/(1.5 La + Zn) molar ratio at 1.25 in all cases. The resulting materials were designated La[0]Zn[100], La[1]Zn[99], La[5]Zn[95], La[25]Zn[75], La[50]Zn[50], and La[100]Zn[0].

2.2.2. Coprecipitation of lanthanum and magnesium or calcium

The synthesis of La-doped Mg or Ca hydroxycarbonates was identical to the preparation of La[10]Zn[90] except for the use of $Mg(NO_3)_2{\cdot}6H_2O$ or $Ca(NO_3)_2{\cdot}4H_2O$ instead of $Zn(NO_3)_2{\cdot}6H_2O$. The resulting materials were designated La[10]Mg[90] and La[10]Ca[90].

2.2.3. Material characterization

The crystallinity of the La-containing materials was evaluated by powder X-ray diffraction (XRD) using a Siemens D5000*matic* diffractometer with Ni-filtered Cu$K\alpha$ radiation ($\lambda = 0.1542$ nm). Diffractograms were recorded between $2\theta = 3°$ and $2\theta = 80°$ with a scanning rate of 2θ 0.15° min^{-1}. Fourier transform infrared (FTIR) spectra were recorded on a Nicolet FTIR 730 spectrophotometer using the KBr pellet technique. The spectra were acquired by accumulating 128 scans at a resolution of 2 cm^{-1} in the range of 400–4000 cm^{-1}. Zn and La contents of the solids were determined by inductively coupled plasma (ICP) mass spectrometry at the Soil Service of Belgium (Leuven) after the samples were dissolved in aqueous nitric acid. Thermogravimetric analysis was performed using a Thermal Analysis Q500 thermobalance. Samples (10–20 mg) were heated from room temperature up to 800 °C at a heating rate of 5 °C min^{-1} under a nitrogen gas atmosphere. Electron micrographs were obtained using a Philips XL30 FEG scanning electron microscope. N_2 adsorption and desorption isotherms were measured on a TriStar 3000 gas adsorption analyzer from Micromeritics. Before analysis, the samples were dried under a N_2 flow for 10 h at 150 °C. To determine the basic properties of the La-doped catalysts, 0.15 g of the material was dried at 150 °C for 15 h and suspended in 2 mL of an indicator solution (0.1 mg of bromothymol blue or phenolphthalein per mL of dry toluene). These suspensions were stirred for 0.5 h and were titrated with a solution of benzoic acid (0.01 M) in toluene [15].

2.2.4. Detection of the IR chemiluminescence of $^1O_2$ at 1270 nm

Near-infrared emission of $^1O_2$ at 1270 nm was measured with a liquid nitrogen-cooled germanium photodetector (model EO-817L, North Coast Scientific Corp., Santa Rosa, CA) sensitive in the spectral region of 800–1800 nm with a detector of 0.25 cm^2 and a sapphire window. The detector was connected to a lock-in amplifier (Stanford Research Systems, model SR830 DSP) and was powered by a bias supply (North Coast Scientific Corp., model 823A).

A typical chemiluminescence experiment was carried out as follows. A suspension containing the La[5]Zn[95] catalyst

(0.1 g) in methanol (10 mL) was stirred at 40 °C, and the mixture was pumped continuously through a quartz cell placed in front of the germanium detector. Once the background noise of the IR signal was stable, 5 mmol H_2O_2 (50 wt%) was introduced. The intensity of the signal at 1270 nm was recorded as a function of time. The maximum intensity of the signal is related to the rate of $^1O_2$ generation, and the total area under the curve is directly related to the cumulated amount of singlet oxygen. The yield of $^1O_2$ generated from the La[5]Zn[95] catalyst was determined by comparing the total area under the signal curve with that obtained for the Na_2MoO_4/H_2O_2 system under similar reaction conditions. For the latter system, it has been shown that the $^1O_2$ yield is 70% in methanol [9,16].

2.3. Catalytic experiments

2.3.1. Disproportionation of hydrogen peroxide

A typical reaction mixture consisted of 10 mL of methanol, 0.1 g of catalyst, and 5 mmol H_2O_2 (50 wt%). The reaction mixture was stirred at 40 °C. H_2O_2 concentrations were determined by cerimetric titration [22]. Small aliquots (200 μL) of the reaction mixture were diluted into 20 mL of water containing 2 mL of aqueous H_2SO_4 (7 vol%). The mixture was titrated with 0.1 M $Ce(SO_4)_2{\cdot}4H_2O$ in aqueous H_2SO_4 (1 M) until the color of the solution changed to yellow.

2.3.2. Oxidation of citronellol

In a typical experiment, a 25-mL flask was charged with 10 mL of methanol, 0.2 g of catalyst, 10 mmol of β-citronellol, and 20 mmol of H_2O_2 (50 wt%), and the reaction mixture was stirred at 40 °C. The concentration of β-citronellol (0.75 M) is well above its β value ($\beta = 0.15$ M in methanol), implying that most of the formed $^1O_2$ is chemically trapped and that the loss of $^1O_2$ via alternative quenching pathways is very small [23]. Gas chromatography (GC) analysis of the reaction mixture was performed after complete H_2O_2 conversion. Before the GC analysis, the solid catalyst was removed by centrifugation, and the hydroperoxides were reduced to the corresponding alcohols using excess trimethylphosphine (1 M) in tetrahydrofuran. A Hewlett Packard 5890 gas chromatograph (Chrompack CP-Sil 5 CB fused silica WCOT column, 30 m × 0.32 mm × 1 μm) equipped with a flame ionization detector was used for this.

2.3.3. Heterogeneity and catalyst reuse

To verify the heterogeneous nature of the observed catalysis, a conventional filtrate test was carried out [24]. Using La[10]Zn[90] as the catalyst, the peroxidation of β-citronellol was carried out under standard conditions. At 30% conversion of β-citronellol (4 h), half of the reaction mixture was filtered at 40 °C. The clear filtrate and the remaining catalyst suspension were further stirred at 40 °C, and the progress of the reaction was monitored by GC analysis.

To study the recycling of the La-doped zinc hydroxycarbonates, the La[10]Zn[90] catalyst was reused four times in the oxidation of β-citronellol in both the presence and absence of KOH (0.02 M) as a soluble base. The reaction was carried out under standard conditions. After each run, the catalyst was separated by centrifugation, washed with acetone, and dried at room temperature.

Table 1
Chemical composition (ICP-MS analysis) of the La–Zn coprecipitates

Entry	Sample	La/(Zn + La) [mol%]	La [mmol g^{-1}]
1	La[1]Zn[99]	1.1	0.09
2	La[5]Zn[95]	5.1	0.41
3	La[10]Zn[90]	9.9	0.74
4	La[25]Zn[75]	25.9	1.61
5	La[50]Zn[50]	52.6	2.55
6	La[100]Zn[0]	100.0	3.55

2.3.4. Peroxidation of functionalized alkenes

A 25-mL flask was charged with 10 mL of methanol, 10 mmol alkene, 0.2 g of La[10]Zn[90] (0.15 mmol La), and 60–80 mmol H_2O_2 (50 wt%). The reaction mixture was stirred at 40 °C, and the reaction progress was followed by GC analysis of the crude reaction mixture after centrifugation and reduction with excess $(CH_3)_3P$. Products were identified by GC-MS and by comparing the GC retention times with authentic allylic alcohols prepared by photochemical oxidation [19].

3. Results and discussion

3.1. Material characterization

3.1.1. Chemical analysis

A series of La-containing materials with varying La/Zn ratios was prepared by coprecipitation of La^{3+} and Zn^{2+} nitrate salts with sodium carbonate. The metal composition of the resulting materials was determined by ICP mass spectrometry. As shown in Table 1, the La/(Zn + La) ratio of the final materials closely reflects the metal composition of the original synthesis mixture. The lanthanum content varied between 0.1 mmol g^{-1} for La[1]Zn[99] and 3.5 mmol g^{-1} for La[100]Zn[0].

3.1.2. XRD

The XRD diffraction patterns of the synthesized materials are shown in Figs. 1 and 2. The XRD pattern of La[0]Zn[100] corresponds with the powder diffraction data reported for zinc hydroxycarbonates, such as $Zn_4CO_3(OH)_6$ or the mineral hydrozincite, $Zn_5(CO_3)_2(OH)_6$ [25]. The diffraction pattern observed for La[100]Zn[0] shows lower intensity and is less well defined. Presumably, this sample contains a mixture of different phases of normal and basic lanthanum carbonates [26–28]. The XRD patterns of La[1]Zn[99], La[5]Zn[95], and La[10]Zn[90] are very similar to the XRD pattern observed for hydrozincite (Fig. 1). The XRD patterns of La[25]Zn[75] and La[50]Zn[50] are less well defined and resemble the pattern observed for La[100]Zn[0] (Fig. 2). The hydrozincite structure no longer can be recognized with certainty.

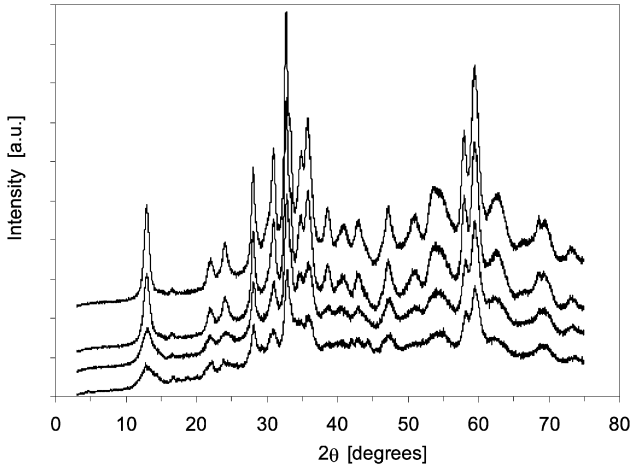

Fig. 1. XRD patterns of La[0]Zn[100] (top), La[1]Zn[99], La[5]Zn[95], and La[10]Zn[90] (bottom).

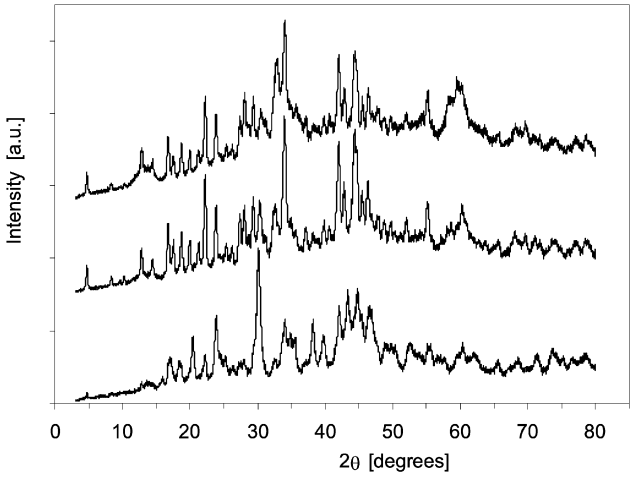

Fig. 2. XRD patterns of La[25]Zn[75] (top), La[50]Zn[50], and La[100]Zn[0] (bottom).

3.1.3. Thermogravimetric analysis

The thermal decomposition profile of La[0]Zn[100] is in good agreement with that reported for zinc hydroxide carbonates such as hydrozincite (Fig. 3) [25]. The weight loss at 200–250 °C corresponds to the transformation of hydrozincite to zinc oxide (ZnO) and the release of CO_2 and H_2O. La[1]Zn[99] and La[5]Zn[95] show similar thermal behavior as La[0]Zn[100]. The La[100]Zn[0] sample shows two distinct weight losses. For the La[10]Zn[90], La[25]Zn[75], and La[50]Zn[50] samples, three weight loss processes are observed.

3.1.4. IR spectroscopy

The FTIR spectrum of La[0]Zn[100] shows a strong, broad absorption band centered at 3360 cm^{-1} (Fig. 4), attributed to the O–H stretching vibrations of nonstructural water molecules. The stretching vibrations corresponding to structural hydroxyl groups in the hydrozincite La[0]Zn[100], which contribute to the IR band at 3360 cm^{-1}, are not resolved. The spectrum clearly indicates the presence of carbonate groups. The two strong bands at 1500 and 1380 cm^{-1} are assigned to the two

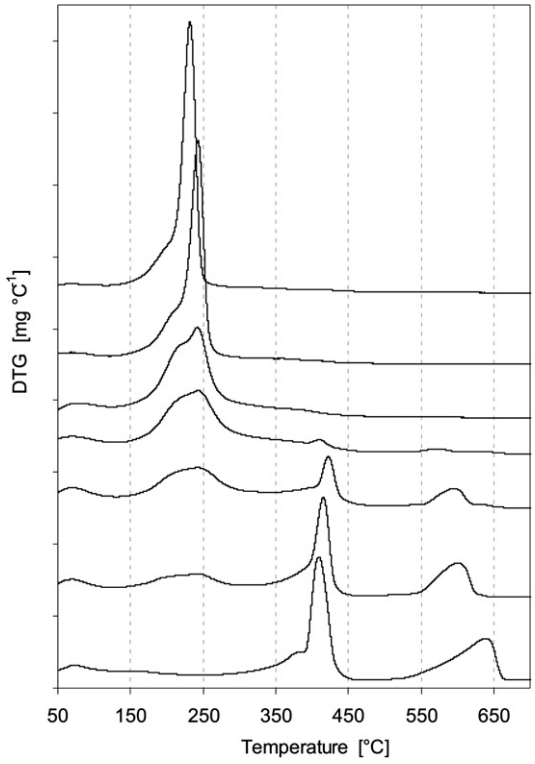

Fig. 3. DTG profiles of La[0]Zn[100] (top), La[1]Zn[99], La[5]Zn[95], La[10]Zn[90], La[25]Zn[75], La[50]Zn[50], and La[100]Zn[0] (bottom).

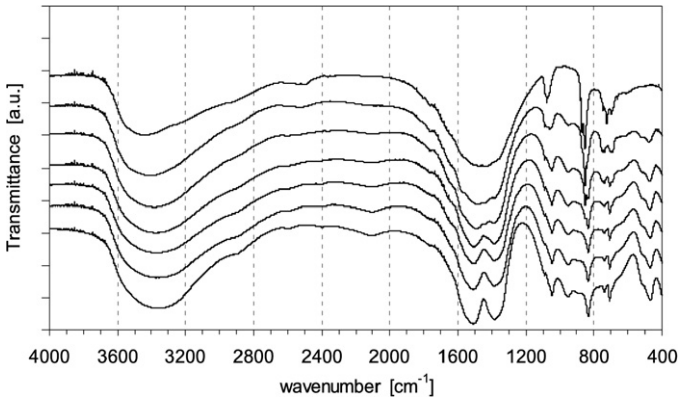

Fig. 4. FT-IR spectra of La[100]Zn[0] (top), La[50]Zn[50], La[25]Zn[75], La[10]Zn[90], La[5]Zn[95], La[1]Zn[99], and La[0]Zn[100] (bottom).

components of the asymmetric C–O stretching vibration (ν_3) of the carbonate anion [29,30]. The weak band at 1070 cm^{-1} (shoulder) is probably due to the symmetric C–O stretching mode (ν_1). The strong band at 830 cm^{-1} is characteristic of the out-of-plane OCO bending vibration of CO_3^{2-} (ν_2), whereas the bands at 740 and 710 cm^{-1} are attributed to the two components of the in-plane OCO bending mode (ν_4). The bands at 1050 and 950 cm^{-1} in the spectrum of La[0]Zn[100] are assigned to OH bending vibrations. In the IR spectrum of La[100]Zn[0], the four vibration modes of the CO_3^{2-} ion appear at 1080 cm^{-1} (ν_1), 860 cm^{-1} (ν_2), 1450 cm^{-1} (ν_3), and 720 cm^{-1} (ν_4). The stretching band of hydrogen-bonded OH groups or nonstructural water is observed at 3440 cm^{-1}.

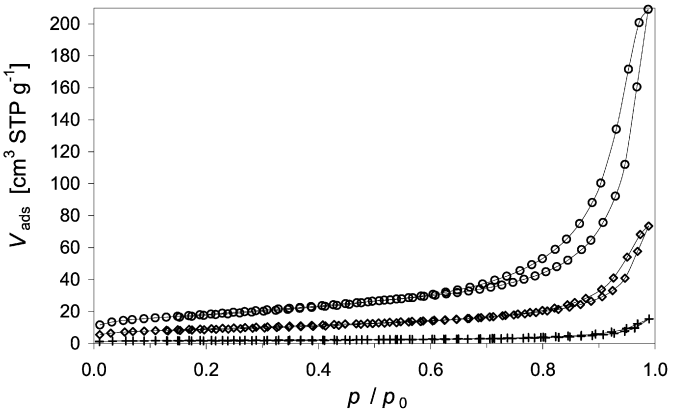

Fig. 5. N_2 adsorption isotherms of La[10]Zn[90] (top), La[10]Mg[90], and La[10]Ca[90] (bottom).

3.1.5. Nitrogen gas adsorption

N_2 adsorption isotherms of the La–Zn, La–Mg, and La–Ca materials are shown in Fig. 5. The derived BET surface areas were 64.3 $m^2\,g^{-1}$ for La[10]Zn[90], 31.9 $m^2\,g^{-1}$ for La[10]Mg[90], and 6.5 $m^2\,g^{-1}$ for La[10]Ca[90]. The corresponding total pore volumes were 0.32, 0.11, and 0.02 $cm^3\,g^{-1}$ at $p/p_0 = 0.99$. Clearly, the La–Zn material has the largest surface area and the highest total pore volume.

3.1.6. Scanning electron micrographs

Fig. 6 shows the corresponding scanning electron micrographs for these materials. The La[10]Ca[90] material consists of rod-like secondary structures and individual crystals of about 0.5 μm in size. La[10]Mg[90] shows porous aggregates consisting of relatively large crystallites with platy morphology. The La[10]Zn[90] material consists of crystals of very small size.

3.1.7. Basic properties of La-doped Ca, Mg, and Zn materials

To assess the basic properties of the La–Zn, La–Mg, and La–Ca materials, the number and the strength of the basic sites were determined by titration with benzoic acid in the presence of bromothymol blue or phenolphthalein as the pH indicator [15,31]. Toluene was used as the solvent to disperse the predried solids (15 h at 150 °C). As shown in Table 2, both the number of weak and strong basic sites (as measured in the titration with bromothymol blue, $pK_a = 7.1$) and the number of the stronger basic sites (measured with phenolphthalein as indicator, $pK_a = 9.3$) increased in the order La[10]Ca[90] < La[10]Mg[90] < La[10]Zn[90]. These results show that the La-doped zinc hydroxycarbonate contains a high number of easily accessible basic sites of relatively high basic strength.

Summarizing, Zn–La coprecipitates with low La content, such as La[1]Zn[99], La[5]Zn[95], and La[10]Zn[90], can be considered hydrozincites doped with a small amount of La,

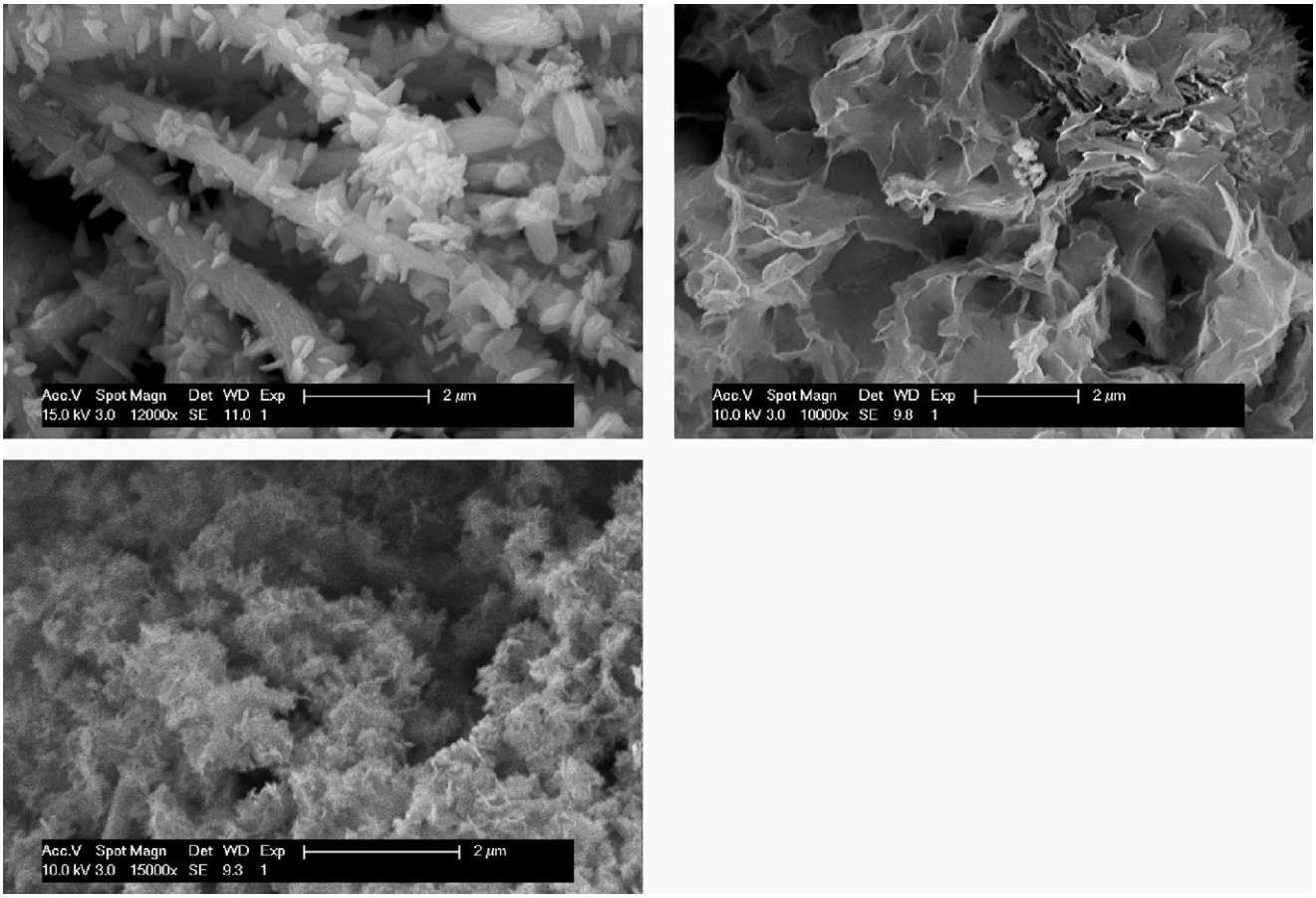

Fig. 6. SEM micrographs of La[10]Ca[90] (top left), La[10]Mg[90] (top right), and La[10]Zn[90] (bottom).

Table 2
Determination of the basic properties of La-doped Ca, Mg, and Zn catalysts

Entry	Sample	mmol basic sites per g of catalyst[a]	
		Bromothymol blue ($pK_a = 7.1$)	Phenolphthalein ($pK_a = 9.3$)
1	La[10]Ca[90]	0.017	0.010
2	La[10]Mg[90]	0.097	0.089
3	La[10]Zn[90]	0.276	0.272

[a] A suspension of 0.15 g of the predried solid (15 h at 150 °C) in 2 mL of toluene containing the indicator (0.1 mg mL^{-1}) was stirred for 0.5 h and was titrated with benzoic acid (0.01 M) in toluene. The titration experiments were carried out twice or thrice and good reproducibility was obtained in all cases (uncertainty < 5%).

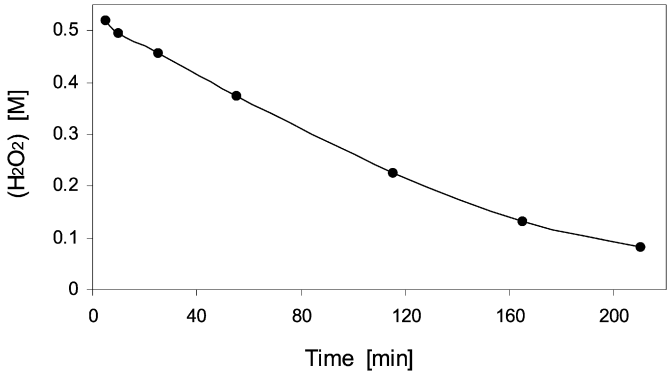

Fig. 7. Disproportionation of H_2O_2 in the presence of La[10]Zn[90]. Reaction conditions: 0.1 g of La[10]Zn[90] (0.075 mmol La), 10 mL of MeOH, 5 mmol H_2O_2 (50 wt%), 40 °C. H_2O_2 determination by cerimetry.

which may be deposited on the structure or substituted into it. The La[10]Zn[90] material has a relatively large surface area, small crystal size, and a high number of easily accessible basic sites. For materials with higher La content, the hydrozincite structure no longer can be recognized with certainty; these materials bear a resemblance to La (hydroxy)carbonates.

3.2. Catalytic performance

3.2.1. Disproportionation of H_2O_2

The lanthanum-containing materials were tested for their catalytic activity in the disproportionation of H_2O_2. The rate of H_2O_2 disappearance was determined by cerimetric titration. A typical kinetic profile of the disproportionation of H_2O_2 in the presence of La[10]Zn[90] is shown in Fig. 7. H_2O_2 disproportionation rates were calculated from the initial linear region of the $[H_2O_2]$ versus time plots. It is assumed that the rate thus obtained is directly related to the rate of $^1O_2$ generation. The initial reaction rates of all La catalysts tested are compiled in Tables 3 and 4. The activity data are presented on a weight basis ($mmol_{HOOH}\ g_{cat}^{-1}\ s^{-1}$). For the materials with known La content, catalytic activities on a mole basis (turnover frequencies, s^{-1}) are also shown.

The results in Table 3 indicate that the La-doped Zn hydroxycarbonate is an active catalyst for the disproportionation of H_2O_2 (entry 1). In contrast, La-doped Mg or Ca materials are almost fully inactive under these reaction conditions (entries 2 and 3). Note that $Ca(OH)_2$ has been reported as a catalyst for the generation of $^1O_2$ from H_2O_2 [32]. Immobilization of lanthanum on other basic supports, such as hydrotalcite, yielded materials with low catalytic activity. La-containing solids, such as $La(OH)_3$, showed moderate activity in the disproportionation of H_2O_2 (entry 4). Finally, La_2O_3 showed virtually no activity (entry 5).

Table 3
Disproportionation of H_2O_2 catalyzed by lanthanum-containing solids[a]

Entry	Catalyst	Initial rate of H_2O_2 disproportionation	
		$[mmol_{HOOH}\ g_{cat}^{-1}\ s^{-1}]$[b]	$[s^{-1}]$[c]
1	La[10]Zn[90]	0.43	0.59
2	La[10]Mg[90]	0.01	–
3	La[10]Ca[90]	0.02	–
4	$La(OH)_3$	0.12	0.022
5	La_2O_3	0.02	0.003

[a] Reaction conditions: 0.1 g of La catalyst, 10 mL of MeOH, 5 mmol H_2O_2 (50 wt%), 40 °C.
[b] Activity per g of catalyst.
[c] Activity per mole of lanthanum.

Table 4
Disproportionation of H_2O_2 catalyzed by La-containing Zn hydroxycarbonates[a]

Entry	Catalyst	Initial rate of H_2O_2 disproportionation[b]	
		$[mmol_{HOOH}\ g_{cat}^{-1}\ s^{-1}]$[c]	$[s^{-1}]$[d]
1	La[0]Zn[100]	0.02	–
2	La[1]Zn[99]	0.13 (0.30)	1.48 (3.33)
3	La[5]Zn[95]	0.40 (0.93)	0.98 (2.28)
4	La[10]Zn[90]	0.43 (1.00)	0.59 (1.35)
5	La[25]Zn[75]	0.33 (0.80)	0.21 (0.50)
6	La[50]Zn[50]	0.27 (0.73)	0.10 (0.29)
7	La[100]Zn[0]	0.20 (0.70)	0.06 (0.20)
8[e]	La[0]Zn[100] + La[100]Zn[0]	0.03	–

[a] Reaction conditions: 0.1 g of La catalyst, 10 mL of MeOH, 5 mmol H_2O_2 (50 wt%), 40 °C.
[b] Values between brackets are for reactions in the presence of 0.02 M KOH in methanol.
[c] Activity per g of catalyst.
[d] Activity per mole of lanthanum.
[e] Physical mixture of 0.09 g of La[0]Zn[100] and 0.01 g of La[100]Zn[0].

The observed difference in catalytic activity among La[10]Zn[90], La[10]Ca[90], and La[10]Mg[90] may be attributed to the greater surface area, smaller crystal size, and higher number of easily accessible basic sites of La[10]Zn[90] (Table 2; Figs. 5 and 6). The differences in surface area and basicity are less pronounced for the La–Mg material.

Because of its promising catalytic properties, the La–Zn coprecipitate was studied in more detail. A series of La-containing Zn hydroxycarbonates with La/Zn ratios varying between 0/100 and 100/0 was prepared, and the resulting materials were tested in the disproportionation of H_2O_2 (Table 4). The activity of these La catalysts was strongly dependent on the relative amount of La that is introduced in the material (Fig. 8). The highest activities on a weight basis were observed for catalysts containing a relatively small amount of La, such as La[5]Zn[95] and La[10]Zn[90] (entries 3 and 4). The highest catalytic activity on a mole basis was observed for La[1]Zn[99], but relatively large amounts of this catalyst were required to obtain acceptable activity on a weight basis (entry 2). The most

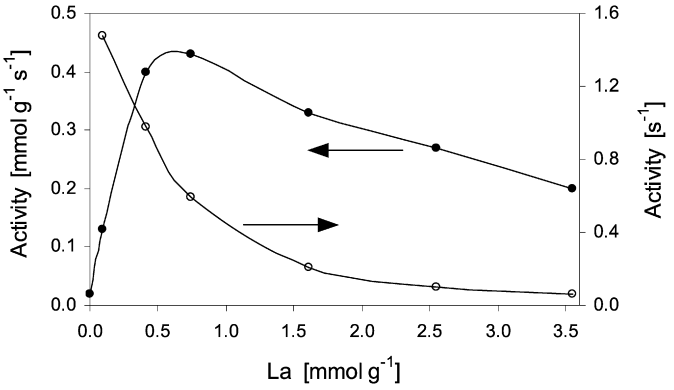

Fig. 8. Initial rate of H_2O_2 disproportionation ($mmol_{HOOH}\ g_{cat}^{-1}\ s^{-1}$) and La turnover frequency (s^{-1}) versus La content of La–Zn coprecipitates with varying La/Zn ratio. Reaction conditions as in Table 4.

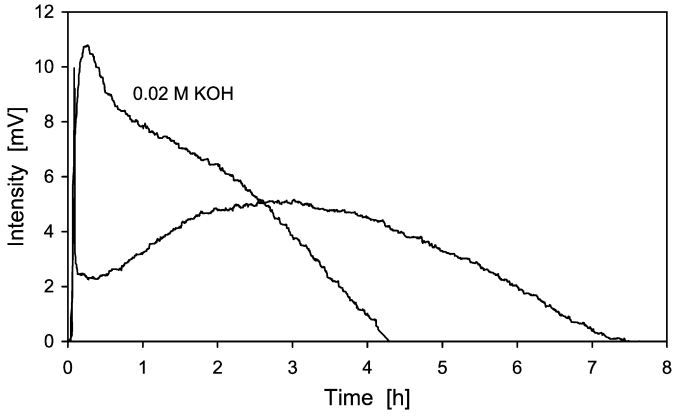

Fig. 9. Chemiluminescence signal (1270 nm) of singlet oxygen generated from a suspension containing La[5]Zn[95] and H_2O_2 in methanol in the absence or presence of 0.02 M KOH. Reaction conditions: 0.1 g of La[5]Zn[95], 0 or 0.02 M KOH in 10 mL of MeOH, 5 mmol H_2O_2 (50 wt%), 40 °C.

active catalysts on a mole basis were the La-doped hydrozincites. In contrast, the La (hydroxy)carbonate phases formed at high La loading were less active, presumably because most of the lanthanum is buried in the inactive bulk phase. Materials containing no lanthanum, such as La[0]Zn[100], showed negligible activity in the disproportionation of H_2O_2 (entry 1). A physical mixture of La[0]Zn[100] and La[100]Zn[0] containing the same amount of La as La[10]Zn[90] showed very low activity (entry 8).

For all materials, the addition of a catalytic amount of a base (0.02 M KOH in methanol) had a beneficial effect on activity (Table 4). However, in contrast with other La catalysts [18,19], the La–Zn coprecipitates were able to produce $^1O_2$ in the absence of an additional soluble base, such as KOH.

3.2.2. Detection of the chemiluminescence of $^1O_2$ at 1270 nm

The IR chemiluminescence of the weak radiative transition of $^1O_2$ at 1270 nm was used as specific and unequivocal proof of the formation of singlet ($^1\Delta_g$) molecular oxygen in the disproportionation of H_2O_2 catalyzed by the La-doped Zn hydroxycarbonates [33],

$$^1O_2(^1\Delta_g) \rightarrow {}^3O_2(^3\Sigma_g^-) + h\nu \quad (\lambda = 1270\ \text{nm}).$$

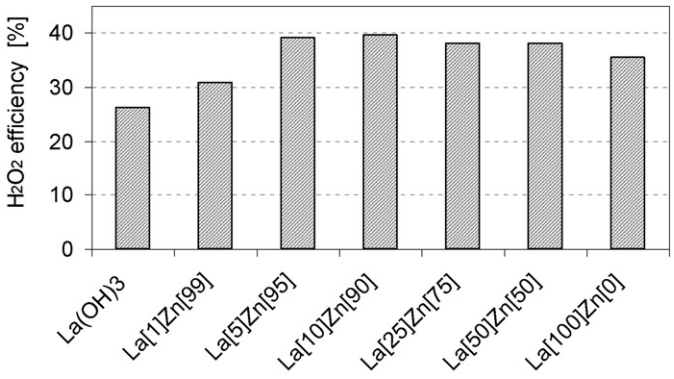

Fig. 10. H_2O_2 efficiency of La-containing materials in the oxidation of β-citronellol. Reaction conditions: 0.2 g of La catalyst, 10 mmol β-citronellol, 10 mL of MeOH, 20 mmol H_2O_2 (50 wt%), 40 °C, 48 h. GC analysis after centrifugation and reduction with excess $(CH_3)_3P$ (uncertainty < 2%). The H_2O_2 efficiency is defined as $[mol_{hydroperoxides}\ mol_{HOOH}^{-1}\ 0.5)] \times 100$.

Table 5
Peroxidation of functionalized alkenes with La[10]Zn[90] and H_2O_2[a]

Entry	Substrate	Products distribution [%]	H_2O_2 [eq.]	Conv. [%]	Sel.[b] [%]
1	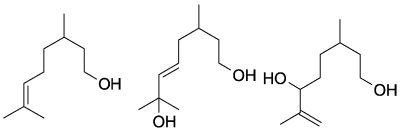		6	89.6	96.7
2[c]				90.0	97.2
3[d]				89.5	96.8
4			8	97.8	91.9
5[c]		50 50		98.7	94.8
6	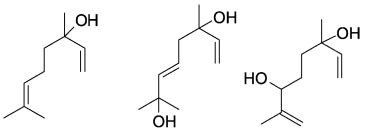		6	80.0	99.0
7			8	96.1	99.0
		47 53			
8	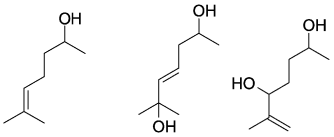		8	91.1	99.0
		48 52			

[a] Reaction conditions: 0.2 g of La[10]Zn[90] (0.15 mmol La), 10 mmol alkene, 10 mL of MeOH, 60–80 mmol H_2O_2 (50 wt%), 40 °C, 24 h. GC analysis after centrifugation and reduction with excess $(CH_3)_3P$.
[b] Selectivity to allylic alcohols.
[c] 10 mL of 0.02 M KOH in MeOH.
[d] 0.2 g of La[5]Zn[95] (0.08 mmol La), 10 mL of 0.02 M KOH in MeOH.

Fig. 9 clearly demonstrates that the disproportionation of H_2O_2 catalyzed by the La[5]Zn[95] catalyst resulted in the formation of singlet ($^1\Delta_g$) molecular oxygen. The amount of $^1O_2$ generated, as determined from the chemiluminescence experiments (37%), is in good agreement with the H_2O_2 efficiency assessed from the peroxidation of citronellol (39%; Fig. 10). Thus, the disproportionation of H_2O_2 in the presence of La-doped zinc hydroxycarbonates produced singlet oxygen as a principal oxidizing species. The characteristic products and the unique product distribution observed in the reaction of singlet oxygen with alkyl-substituted olefins further indicate that $^1O_2$ was the only

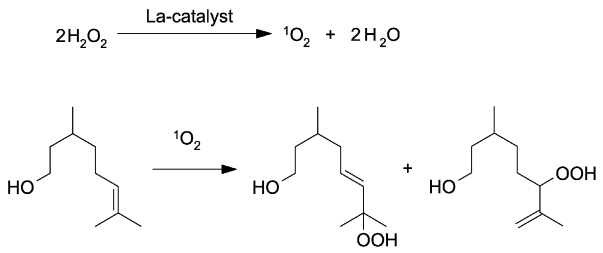

Scheme 1. Generation of $^1O_2$ and its reaction with β-citronellol.

oxidizing species involved (Table 5). The mixture of allylic alcohol products showed the same product distribution as that observed for photochemical oxidation in solution. This product distribution differed significantly from that in other types of oxidation, such as oxidation by radical species (e.g., HO°, $O_2^{-\circ}$). Both observations indicate that $^1O_2$ was the main oxidizing species.

3.2.3. Determination of the $^1O_2$ yield by chemical trapping with citronellol

The amount of singlet oxygen produced from the La-catalyzed disproportionation of H_2O_2 was assessed by chemical trapping of $^1O_2$ with β-citronellol, a typical olefinic substrate. Reaction of $^1O_2$ with β-citronellol yielded an equimolar mixture of isomeric allylic hydroperoxides (Scheme 1). These products and the product distribution are characteristic of the peroxidation of citronellol via a singlet oxygenation pathway. Quantification of the formed allylic hydroperoxides by GC analysis allows the assessment of H_2O_2 efficiency, which fully corresponds to the $^1O_2$ yield if all formed $^1O_2$ is trapped by β-citronellol. Because singlet oxygen is also lost through alternative quenching processes (e.g., physical quenching by the solvent, substrate, or solid catalyst), the yield obtained in the oxidation of citronellol is somewhat lower than the actual amount of $^1O_2$ released by the catalyst. Nonetheless, the citronellol yield gives a fair estimate of the amount of $^1O_2$ available for a synthetically useful reaction with an organic substrate.

The H_2O_2 efficiencies of the different La catalysts in the oxidation of β-citronellol are shown in Fig. 10. Materials showing very low activity in the disproportionation of H_2O_2 (Table 3) were not tested in the oxidation of citronellol. The reaction was run for an extended period (48 h) to allow complete H_2O_2 disproportionation for most of the catalysts. But even after 48 h, incomplete H_2O_2 decomposition was observed for $La(OH)_3$, La[1]Zn[99], and La[100]Zn[0]. This might explain the lower H_2O_2 efficiency observed for these catalysts. The La-doped Zn hydroxycarbonates La[5]Zn[95] and La[10]Zn[90] showed H_2O_2 efficiencies of around 40%. Similar conversions and selectivities were obtained for La[10]Zn[90] in the presence of 0.02 M KOH. On the other hand, La[25]Zn[75] and La[50]Zn[50] showed slightly lower conversion in the oxidation of β-citronellol. The selectivity toward the expected allylic alcohols was 94–95% in all cases. For La[1]Zn[99] and $La(OH)_3$, slightly lower selectivity (90%) was observed. Overall, the amount of singlet oxygen produced by the La-containing Zn hydroxycarbonates was much less dependent on the La/Zn ratio than the rate of H_2O_2 disproportionation was (Table 4; Fig. 8). H_2O_2 efficiencies around 40% were observed for most of the catalysts. Presumably, for most of the materials, the formed $^1O_2$ can react with β-citronellol with similar efficiency.

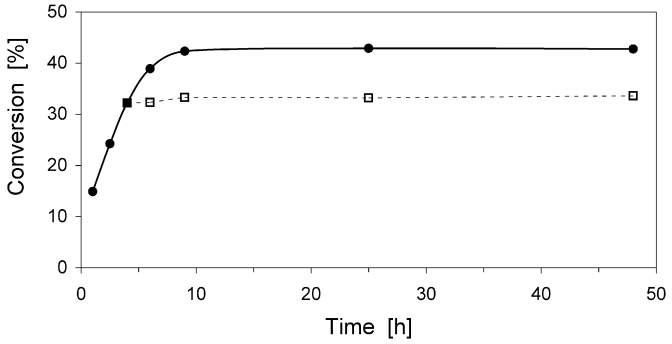

Fig. 11. Conversion of β-citronellol as a function of time in the suspension (●) with La[10]Zn[90] and in the filtrate (□) after catalyst removal. Reaction conditions: 0.2 g of La[10]Zn[90], 10 mmol citronellol, 10 mL of MeOH, 20 mmol H_2O_2 (50 wt%), 40 °C.

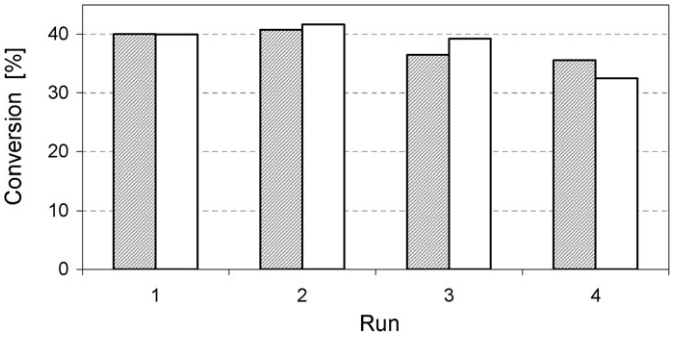

Fig. 12. Reuse of La[10]Zn[90] in the peroxidation of citronellol in the presence (gray boxes) or absence (white boxes) of 0.02 M KOH. Reaction conditions: 0.2 g of La[10]Zn[90], 10 mmol β-citronellol, 0 or 0.02 M KOH in 10 mL of MeOH, 20 mmol H_2O_2 (50 wt%), 40 °C, 24 h.

3.2.4. Heterogeneity and catalyst reuse

To verify whether the observed catalysis was due to the solid La catalyst or to leached lanthanum species, the La[10]Zn[90] catalyst was used for the peroxidation of β-citronellol, and a filtrate test was carried out [24]. After 4 h (32% conversion of β-citronellol), half of the reaction mixture was filtered at 40 °C, and both the clear filtrate and the remaining catalyst suspension were further stirred at 40 °C. As shown in Fig. 11, no further conversion of β-citronellol was observed in the clear filtrate, whereas the reaction proceeded smoothly in the catalyst suspension. Even after 48 h, the conversion of β-citronellol in the filtrate did not increase. On the other hand, as measured by cerimetric titration, the concentration of H_2O_2 in the clear filtrate did not decrease after catalyst removal. These experiments clearly demonstrate the complete absence of any catalytically active La species in solution.

To study the reusability of the La-doped zinc hydroxycarbonates, the La[10]Zn[90] catalyst was reused in four subsequent oxidation reactions of β-citronellol in both the presence and absence of KOH (0.02 M) as a soluble base. After each run, the catalyst was separated by centrifugation, washed with acetone, and dried at room temperature. As shown in Fig. 12, a small decrease in the conversion of β-citronellol was observed

in the third or fourth run. However, the slightly decreasing conversion might be due in part to small losses of catalyst during the subsequent separation and washing steps between the different runs.

3.2.5. Peroxidation of functionalized alkenes

The La[10]Zn[90] catalyst was used for the peroxidation of various functionalized alkenes (Table 5). The oxidation of citronellol with La[10]Zn[90] and 6 eq. of H_2O_2 resulted in 90% conversion after 24 h. The selectivity toward the allylic alcohols was 97% (entry 1). No oxidation of the primary alcohol group and only very limited epoxidation of the double bond were observed. Reaction in alkaline conditions (0.02 M KOH) or the use of La[5]Zn[95] under such pH conditions resulted in nearly identical yields (entries 2 and 3). The addition of 8 eq. of H_2O_2 gave almost complete conversion of citronellol in both the absence and presence of KOH as a soluble base (entries 4 and 5). The product distribution in the oxidation of citronellol did not vary significantly with the degree of conversion, the La content of the catalyst, or the choice of reaction conditions. An almost equimolar mixture of isomeric allylic alcohols was formed in all cases (entries 1–5). The peroxidation of β-citronellol is of particular relevance, because it is the first step in the industrial three-step synthesis of rose oxide, a well-known ingredient used in rose and geranium perfumes [34–36]. Linalool (entries 6 and 7) and 6-methyl-5-hepten-2-ol (entry 8) showed slightly lower reactivity toward singlet oxygen but, as observed for β-citronellol, these substrates were also oxidized with high selectivity. For linalool, a monoterpene containing an allylic alcohol functionality, peroxidation occurred at the isolated electron-rich 6,7-double bond. Epoxidation of the less electron-rich allylic double bond was not observed. Secondary alcohol groups also did not react under these conditions (entry 8), demonstrating the excellent chemoselectivity of the La[10]Zn[90] catalyst.

4. Conclusion

Several lanthanum-containing materials were evaluated for their catalytic activity in the disproportionation of hydrogen peroxide. Whereas La supported on Mg or Ca materials showed almost no catalytic activity, La-doped Zn hydroxycarbonates showed high activity in the disproportionation of H_2O_2, even in the absence of a soluble base. By varying the La/Zn ratio of the La-modified Zn hydroxycarbonates, La[10]Zn[90] was identified as the most active catalyst. This material can be considered a La-doped hydrozincite. This catalyst demonstrated high regioselectivity and chemoselectivity in the peroxidation of functionalized alkenes.

Acknowledgments

Financial support was provided by the European Commission (SUSTOX project, G1RD-CT-2000-00347) and the Belgian Government (IAP project on Supramolecular Chemistry and Catalysis). J.W. acknowledges FWO and the K.U. Leuven Onderzoeksfonds for a postdoctoral fellowship (PDM/04/204).

References

[1] E.L. Clennan, A. Pace, Tetrahedron 61 (2005) 6665.
[2] M. Prein, W. Adam, Angew. Chem. Int. Ed. 35 (1996) 477.
[3] M.C. DeRosa, R.J. Crutchley, Coord. Chem. Rev. 233 (2002) 351.
[4] J. Wahlen, D.E. De Vos, P.A. Jacobs, P.L. Alsters, Adv. Synth. Catal. 346 (2004) 152.
[5] J.-M. Aubry, J. Am. Chem. Soc. 107 (1985) 5844.
[6] K. Böhme, H.-D. Brauer, Inorg. Chem. 31 (1992) 3468.
[7] Q.J. Niu, C.S. Foote, Inorg. Chem. 31 (1992) 3472.
[8] V. Nardello, J. Marko, G. Vermeersch, J.-M. Aubry, Inorg. Chem. 34 (1995) 4950.
[9] V. Nardello, S. Bogaert, P.L. Alsters, J.-M. Aubry, Tetrahedron Lett. 43 (2002) 8731.
[10] J.-M. Aubry, S. Bouttemy, J. Am. Chem. Soc. 119 (1997) 5286.
[11] V. Nardello, L. Caron, J.-M. Aubry, S. Bouttemy, T. Wirth, C. Saha-Möller, W. Adam, J. Am. Chem. Soc. 126 (2004) 10692.
[12] F. van Laar, D. De Vos, D. Vanoppen, B. Sels, P.A. Jacobs, A. Del Guerzo, F. Pierard, A. Kirsch-De Mesmaeker, Chem. Commun. (1998) 267.
[13] B.F. Sels, D.E. De Vos, P.J. Grobet, F. Pierard, A. Kirsch-De Mesmaeker, P.A. Jacobs, J. Phys. Chem. B 103 (1999) 11114.
[14] B.F. Sels, D.E. De Vos, P.J. Grobet, P.A. Jacobs, Chem. Eur. J. 7 (2001) 2547.
[15] F.M.P.R. van Laar, D.E. De Vos, F. Pierard, A. Kirsch-De Mesmaeker, L. Fiermans, P.A. Jacobs, J. Catal. 197 (2001) 139.
[16] J. Wahlen, D.E. De Vos, B.F. Sels, V. Nardello, J.-M. Aubry, P.L. Alsters, P.A. Jacobs, Appl. Catal. A 293 (2005) 120.
[17] V. Nardello, J. Barbillat, J. Marko, P.T. Witte, P.L. Alsters, J.-M. Aubry, Chem. Eur. J. 9 (2003) 435.
[18] J. Wahlen, D. De Vos, S. De Hertogh, V. Nardello, J.-M. Aubry, P. Alsters, P. Jacobs, Chem. Commun. (2005) 927.
[19] J. Wahlen, S. De Hertogh, D.E. De Vos, V. Nardello, S. Bogaert, J.-M. Aubry, P.L. Alsters, P.A. Jacobs, J. Catal. 233 (2005) 422.
[20] J. Wahlen, D.E. De Vos, M.H. Groothaert, V. Nardello, J.-M. Aubry, P.L. Alsters, P.A. Jacobs, J. Am. Chem. Soc. 127 (2005) 17166.
[21] V. Nardello, J.-M. Aubry, D.E. De Vos, R. Neumann, W. Adam, R. Zhang, J.E. ten Elshof, P.T. Witte, P.L. Alsters, J. Mol. Catal. A 251 (2006) 185.
[22] A.I. Vogel, J. Bassett, Vogel's Textbook of Quantitative Inorganic Analysis, Longman, London, 1978.
[23] F. Wilkinson, W.P. Helman, A.B. Ross, J. Phys. Chem. Ref. Data 24 (1995) 663.
[24] R.A. Sheldon, M. Wallau, I.W.C.E. Arends, U. Schuchardt, Acc. Chem. Res. 31 (1998) 485.
[25] Z. Li, X. Shen, X. Feng, P. Wang, Z. Wu, Thermochim. Acta 438 (2005) 102.
[26] J. Sun, T. Kyotani, A. Tomita, J. Solid State Chem. 65 (1986) 94.
[27] Z. Han, Q. Yang, G.Q. Lu, J. Solid State Chem. 177 (2004) 3709.
[28] S. Bernal, G. Blanco, J.J. Calvino, J.A. Pérez Omil, J.M. Pintado, J. Alloys Compd. 408–412 (2006) 496.
[29] S. Music, S. Popovic, M. Maljkovic, D. Dragcevic, J. Alloys Compd. 347 (2002) 324.
[30] D. Stoilova, V. Koleva, V. Vassileva, Spectrochim. Acta Part A 58 (2002) 2051.
[31] K. Tanabe, M. Misono, Y. Ono, H. Hattori, New Solid Acids and Bases, Studies in Surface Science and Catalysis, vol. 51, Elsevier, Amsterdam, 1989.
[32] V. Nardello, K. Briviba, H. Sies, J.M. Aubry, Chem. Commun. (1998) 599.
[33] Q.J. Niu, C.S. Foote, Inorg. Chem. 31 (1992) 3472.
[34] P. Esser, B. Pohlmann, H.-D. Scharf, Angew. Chem. 106 (1994) 2093.
[35] K. Bauer, D. Garbe, H. Surburg, Common Fragrance and Flavor Materials—Preparation, Properties and Uses, Wiley–VCH, Weinheim, 1997, p. 139.
[36] P. Kraft, J.A. Bajgrowicz, C. Denis, G. Fráter, Angew. Chem. 112 (2000) 3106.